This is an open access article published under a Creative Commons Attribution (CC-BY) License, which permits unrestricted use, distribution and reproduction in any medium, provided the author and source are cited.

I&EC research
Industrial & Engineering Chemistry Research

Article

pubs.acs.org/IECR

Hydrothermal Oxidation of Fecal Sludge: Experimental Investigations and Kinetic Modeling

Tobias Hübner,[†,‡] Markus Roth,[†] and Frédéric Vogel*[,†,‡]

[†]Fachhochschule Nordwestschweiz, Hochschule für Technik, Klosterzelgstrasse 2, 5210 Windisch, Switzerland
[‡]Paul Scherrer Institut, 5232 Villigen, Switzerland

ABSTRACT: Hydrothermal oxidation (HTO) provides an efficient technique to completely destroy wet organic wastes. In this study, HTO was applied to treat fecal sludge at well-defined experimental conditions. Four different kinetic models were adjusted to the obtained data. Among others, a distributed activation energy model (DAEM) was applied. A total of 33 experiments were carried out in an unstirred batch reactor with pressurized air as the oxidant at temperatures of <470 °C, oxygen-to-fuel equivalence ratios between 0 and 1.9, feed concentrations between 3.9 and 9.8 mol_{TOC} L^{-1} (TOC = total organic carbon), and reaction times between 86 and 1572 s. Decomposition of the fecal sludge was monitored by means of the conversion of TOC to CO_2 and CO. In the presence of oxygen, ignition of the reaction was observed around 300 °C, followed by further rapid decomposition of the organic material. The TOC was completely decomposed to CO_2 within 25 min at 470 °C and an oxygen-to-fuel equivalence ratio of 1.2. CO was formed as an intermediate product, and no other combustible products were found in the gas. At certain reaction conditions, the formation of unwanted coke and tarlike products occurred. The reaction temperature and oxygen-to-fuel equivalence ratio showed a significant influence on TOC conversion, while the initial TOC concentration did not. Conversion of TOC to CO_2 could be well described with a first-order rate law and an activation energy of 39 kJ mol^{-1}.

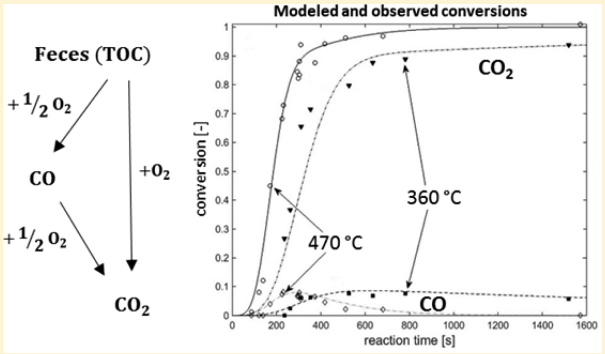

1. INTRODUCTION

According to an estimate of the World Health Organization (WHO) for 2015, approximately 2.4 billion people worldwide have no access to hygienically safe sanitation facilities. The lack of a safe sanitation infrastructure is especially encountered in rural areas of low-income countries and in informal urban settlements (slums). Problems that arise from the lack of sanitation are, for example, contamination of drinking water, the promotion of diseases, and high infant mortalities.[1] Decentral collection and treatment of the fecal matter could provide a solution for this problem. Because a supply of electric energy might be scarce in the target regions, treatment technologies that work "off the grid" are necessary. Hydrothermal oxidation (HTO) could provide a technology that allows safe in situ sanitation of fecal matter and does not require an external infrastructure.

HTO is a process by which organic material is subjected to temperatures between ca. 300 and 700 °C and pressures between ca. 24 and 44 MPa in the presence of an oxidant and water. The material is rapidly decomposed to carbon dioxide (CO_2), ammonia (NH_3), water (H_2O) and its mineral components.[2,3] Pure gaseous oxygen (O_2), air, and hydrogen peroxide (H_2O_2) have been mostly used as oxidants.[3]

The term supercritical water oxidation is used for HTO processes performed at thermodynamic conditions above the critical point of water (374 °C, 22.1 MPa).[2,4]The term wet air oxidation is commonly used for processes performed in liquid water at lower temperatures and pressures.[5−7]

Fecal matter is a semisolid waste product of human digestion consisting of H_2O (63−86%), organic compounds (84−93% of total solids), and inorganic salts (7−16% of total solids). The organic fraction (volatile solids, VS) of fecal sludge contains bacteria (25−54% of VS), carbohydrates (5−25% of VS), proteins and nitrogen-containing compounds (2−25% of VS), lipids (9−16% of VS) and fiber (<25% of VS).[8,9]

During HTO, biomass polymers, such as polysaccharides, proteins, and fats, are hydrolyzed into their oligomers and monomers[10,11] which are subsequently oxidized.[12−14] Price[15] investigated HTO of a mixture of fecal sludge and urine in a continuous reactor system. O_2 was used as the oxidant. Conversions of total organic carbon (TOC) ranged from 80−96.3% at 24 min of residence time and 280−300 °C to 87−93% at 3−5 min of residence time and 400−440 °C. Takahashi and co-workers[16,17] investigated HTO of fecal matter using a stirred cylindrical batch reactor. After 1 h, total conversion of the chemical oxygen demand (COD) was achieved at supercritical conditions (375−450 °C), while 30%, 75%, and 90% conversion were

Received: August 15, 2016
Revised: October 17, 2016
Accepted: October 17, 2016
Published: October 17, 2016

 © 2016 American Chemical Society

DOI: 10.1021/acs.iecr.6b03084
Ind. Eng. Chem. Res. 2016, 55, 11910−11922

achieved at 250, 300, and 350 °C, respectively. Under subcritical conditions, total removal of COD was only possible when a catalyst was applied (gold, palladium, platinum, rhodium, or ruthenium). The work of Jagow[18] confirms these findings. He compared HTO of fecal waste in a continuously stirred tank reactor and a packed-bed reactor at temperatures between 230 and 340 °C using air as the oxidant. He showed that the TOC conversion could be raised from 70−90% to >98% by the application of a catalyst at subcritical conditions. Takahashi et al.[16] also showed that amine-derived nitrogen contained in fecal matter is converted mainly to NH_3 at temperatures of <550 °C. At temperatures of >600 °C, the main part of nitrogen is converted to dinitrogen (N_2) and nitrous oxide. Miller et al.[19] investigated supercritical water oxidation of a model fecal sludge in a continuous reactor system. They examined different process parameters such as the reactor inlet temperature (500−600 °C), solids concentration of the feed (5−8% by weight), reactor pressure, and oxygen-to-fuel equivalence ratio (1.3−1.5). They found that the latter had the greatest influence on their process.

In this study, the treatment of fecal sludge by HTO was investigated at well-defined experimental conditions. The aim was to obtain a kinetic model that is able to accurately predict fecal sludge decomposition over the tested range of experimental conditions for the development of a prototype application. Conversion of TOC to its gaseous oxidation products CO_2 and carbon monoxide (CO) was measured under varying reaction conditions: reaction temperature, reaction time, oxygen-to-fuel equivalence ratio, and feces dilution (or feed concentration). The data were used to adjust the kinetic parameters for four different reaction models. The obtained best-fit parameters of those models were compared to each other and to literature values of similar materials.

2. MATERIALS AND METHODS

2.1. Composition of the Fecal Sludge. The fecal sludge used in this study was obtained from the Swiss Federal Institute of Aquatic Science and Technology, EAWAG, Dübendorf, Switzerland, collected from a diversion toilet. Urine and other material (e.g., toilet paper) were not mixed with the sludge. After a 3-month collection period, the material was homogenized using a kitchen mixer and deep-frozen in freezer bags in portions of 250 g.

Three random samples were taken from the thawed material and analyzed (Table 1). Parts of the samples were dried to constant weight using an LP16 thermogravimetric moisture analyzer (Mettler Toledo, Greifensee, Switzerland). The ash content was determined according to Sluiter et al. (2008) by incinerating dried samples in a muffle furnace at a maximum temperature of 575 °C for 3 h[20] (two repetitions per sample). The higher heating value (HHV) of the dried samples was determined using an IKA C1 bomb calorimeter (Cole-Parmer, USA; three repetitions per sample). The carbon, hydrogen, and sulfur contents of the wet fecal sludge were determined using a Vario ElCube elemental analyzer (Elementar, Germany; five repetitions per sample). The carbon, hydrogen, and nitrogen contents of the dried material were measured by a TrueSpec Micro elemental analyzer. The oxygen content was measured by a RO-487 analyzer and the sulfur content by a CHNS-932 analyzer (Leco, USA; two repetitions per sample).

Most of the obtained results are in good agreement with the literature data of feces composition.[8,9] The measured HHV is higher than the average feces HHV reported in the literature (17.2 MJ kg^{-1}).[9] Feces used in this study originate most likely from a protein-rich nutrition that especially affects their HHV and nitrogen contents. We note that the composition of feces encountered in developing countries might be substantially different, presumably exhibiting lower HHVs.

Table 1. Chemical Composition of the Fecal Sludge Used in This Study[a]

		as received	dried at 105 °C (total solids)
water content	% by weight	74.4 ± 0.8	
total solids	% by weight	25.6 ± 0.8	100
ash	% by weight	3.8[d]	14.8 ± 0.3
HHV	MJ kg^{-1}	5.8 ± 0.01[b,d]	22.7 ± 0.3
LHV	MJ kg^{-1}	3.6[b,c,d]	21.1[b,c]
TOC	% by weight	11.8[d,e]	46.1 ± 0.8
C	% by weight	13.0 ± 0.1	48.6 ± 0.7
H	% by weight		7.1 ± 0.1
N	% by weight	1.38 ± 0.01	5.0 ± 0.1
O	% by weight		27.8 ± 0.5
S	% by weight	0.127 ± 0.003	0.40 ± 0.04
ξ	mol_{O_2} kg^{-1}	12.1 ± 0.4[f,d]	47.1 ± 0.7[f]

[a]Uncertainty expressed as standard deviations from repetitions. Calculation basis: [b]HHV of the dried material. [c]Hydrogen content of the dried material. [d]Water content of the wet material. [e]TOC content of the dried material. [f]Equation 2.

2.2. Batch Reactor Setup and Experimental Procedure. For the experiments, an unstirred cylindrical batch reactor (length, 152.5 mm; inner diameter, 13.5 mm; volume, 24.7 mL) made of 316 L stainless steel (HIP, USA) was used (Figure 1, left). The reactor was heated by immersion into a preheated fluidized sand bath (Techne SBL-2D). The sand was fluidized using pressurized air to achieve rapid heating of the reactor. A stainless steel capillary was attached to the reactor connecting a pressure sensor, a relief valve, and a valve for charging the reactor with pressurized synthetic air. The reaction temperature was measured by a thermocouple situated 14 mm above the reactor bottom (i.e., in the liquid or supercritical reaction phase), except for experiments labeled "Midtemp", in which the reaction temperature was measured in the middle of the reactor (i.e., in the gas phase or supercritical reaction phase).

The upper measuring and charging section of the reactor remained unheated throughout the experiment. The resulting unheated dead volume was 6.6 mL (ca. 21% of the total reactor volume). The influence of this dead volume on the reaction was assumed to be small because oxygen that stayed inside this region was considered not to be accessible for the reaction. This assumption was verified by a test experiment in which a substoichiometric amount of oxygen was supplied ($\lambda < 1$). After a reaction time sufficient for complete oxidation (30 min, 470 °C; i.e., all oxygen should have been consumed by the reaction), the product gas contained approximately the same amount of oxygen that was calculated to fit into the dead volume, whereas the fecal sludge sample was not fully oxidized. We presume that a liquid water droplet condenses inside the steel capillary during reactor heat-up, blocking mass transport between the hot reaction chamber and the dead volume.

For each experiment, a defined amount (0.8−1.4 g) of wet fecal sludge was weighed into the reactor. For dilution of the initial TOC content, additional distilled water was added to the reactor. The reactor was charged with pressurized synthetic air (19.15 ± 0.08 mol % O_2 in N_2). The oxygen-to-fuel equivalence ratio (eq 3) was set by adjusting the ratio of supplied air pressure to the amount of dry fecal mass in the reactor. The reactor was

DOI: 10.1021/acs.iecr.6b03084
Ind. Eng. Chem. Res. 2016, 55, 11910−11922

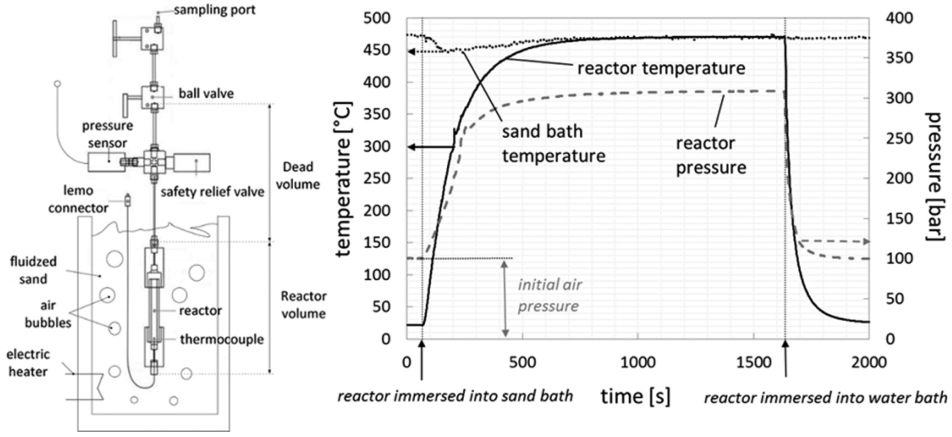

Figure 1. Experimental setup used (left), adapted from Zöhrer,[21] and exemplary temperature and pressure evolution (right).

heated until the desired retention time was reached. To stop the reaction, the reactor was quenched in a water bath. A typical evolution of the pressure and temperature is shown in Figure 1 (right). The heat-up times, defined to reach 95% of the final temperature, were in the range of 6−8 min. The decomposition of the sludge during the heat-up time was accounted for in the kinetic modeling (eq 11).

As reaction products, a suspension of liquid and solid particles and a gas phase were obtained. The gas was collected in a gas sampling bag. These bags were purged with N_2 and, subsequently, evacuated. This procedure was repeated three times before reuse of each bag. The composition of the product gas (CO_2, CO, CH_4, O_2, N_2, and H_2) was analyzed using an HP 6890 gas chromatograph and a thermal conductivity detector (both Agilent, USA). Helium was used as the carrier gas. For the separation of CO_2, an HP PLOT Q column (30 m × 0.53 mm; 0.40 μm film thickness) made of divinylbenzene−styrene porous polymer was used. For the separation of all other gases, an AT-Molecular Sieve column (30 m × 0.53 mm) was used. The total product gas volume was determined using a 1000 mL gastight syringe (Hamilton, USA). The liquid reaction product of each experiment was drained from the reactor, weighed, and filtered through a syringe filter (0.45 μm pore size). The filtrate was diluted by a factor of 20 or 50. The dissolved organic carbon (DOC) and dissolved inorganic carbon (DIC) of the diluted filtrate were determined using a Dimatoc 2000 TOC analyzer (DIMATEC, Germany). After the reactor was emptied, it was flushed with ca. 15 mL of methanol to remove residual water adhering to the reactor walls. The water content of this methanol phase was analyzed by Karl Fischer titration (37 KF coulometer by Metrohm, Switzerland). Using this method, the water mass balance was closed to approximately 80−90%.

2.3. Experimental Design. The reproducibility of the experiments was tested at one set of fixed experimental conditions. The experiment was repeated three times at the standard conditions: 5 min (300 s) of reaction time, 470 °C sand-bath temperature, an oxygen-to-fuel equivalence ratio of 1.2, and 10.0 MPa initial air pressure using undiluted fecal sludge ($c_{TOC,0}$ = 9.8 mol_{TOC} L^{-1}).

For the kinetic experiments, the reaction times were varied between 1.5 and 26 min (86−1572 s) at two different sand-bath temperatures (360 and 470 °C), keeping the other standard conditions constant. The reaction times were chosen to yield reasonably distributed conversions over the range of 0−99%. The TOC concentration of the feed (3.9−9.8 mol_{TOC} L^{-1}) and the oxygen-to-fuel equivalence ratio (0−1.92) were varied and the other parameters fixed to standard reaction conditions.

2.4. Oxygen-to-Fuel Equivalence Ratio. The overall equation for the total oxidation of organic matter, assuming nitrogen-bearing organic compounds to be converted to NH_3, is

$$C_\alpha H_\beta O_\gamma N_\delta + \left(\alpha + \frac{\beta - 3\delta}{4} - \frac{\gamma}{2}\right)O_2 \rightarrow \alpha CO_2 + \left(\frac{\beta - 3\delta}{2}\right)H_2O + \delta NH_3 \quad (1)$$

Accordingly, the stoichiometric amount of oxygen needed for complete oxidation, ξ (mol_{O_2} $kg_{total\ solids}^{-1}$) is given by

$$\xi = \left[\frac{w_C}{M_C} + \frac{1}{4}\frac{w_H}{M_H} - \frac{3}{4}\frac{w_N}{M_N} - \frac{1}{2}\frac{w_O}{M_O}\right]\frac{1}{100\%} \quad (2)$$

where w_C, w_H, w_N, and w_O (% by weight) are the mass fractions of biomass-bound carbon, hydrogen, nitrogen, and oxygen of the dried material (total solids), respectively. Their values were taken from Table 1. M_C, M_H, M_N, and M_O (kg mol^{-1}) are their respective molar masses.

During HTO at temperatures of <550 °C, biomass-bound nitrogen is transformed to NH_3.[16,22] Because the maximum reaction temperatures in this study reached 480 °C, we assume NH_3 to be the oxidation end product. If N_2 is assumed as the oxidation end product, as is the case for reaction temperatures above 550 °C, the stoichiometric amount of oxygen needed for complete oxidation is slightly higher than the ξ value calculated by eq 2 (ca. 5% higher for the nitrogen content of the fecal sludge used in this study). The ξ value, as defined by eq 2, is equal to the COD because, in the determination of the COD, NH_3 is also assumed as the final product of nitrogen-bearing organic compounds.

The oxygen-to-fuel equivalence ratio λ is calculated by

$$\lambda = \frac{n_{O_2,0}}{n_{O_2,stoichiometric}} = \frac{n_{O_2,0}}{\xi m_{TS}} \quad (3)$$

where m_{TS} (kg) is the mass of total solids weighed into the reactor and $n_{O_2,0}$ (mol) is the amount of oxygen available for the reaction. $n_{O_2,0}$ was calculated from the initial synthetic air pressure, the oxygen content of the synthetic air, and the reactor volume available for the gas using the van der Waals equation of

DOI: 10.1021/acs.iecr.6b03084
Ind. Eng. Chem. Res. 2016, 55, 11910−11922

state for real gases:

$$p_0 = \frac{n_{O_2,0}\ R\ T_{amb}}{y_{O_2,0}\left(V_{r,eff} - \frac{n_{O_2,0}}{y_{O_2,0}} b^*\right)} - a^*\left(\frac{n_{O_2,0}}{y_{O_2,0} V_{r,eff}}\right)^2 \quad (4)$$

where p_0 (Pa) is the pressure in the reactor after synthetic air filling at ambient temperature T_{amb} (K), R (J mol^{-1} K^{-1}) is the universal gas constant, $y_{O_2,0}$ is the oxygen molar fraction of the used synthetic air, and the van der Waals coefficients for air[23] are $a^* = 135.8 \times 10^{-3}$ Pa m^6 mol^{-2} and $b^* = 0.0364 \times 10^{-3}$ m^3 mol^{-1}. $V_{r,eff}$ (m^3) is the effective reactor volume containing accessible air for the reaction:

$$V_{r,eff} = V_{r,total} - V_{r,dead} - V_{sample} \quad (5)$$

where $V_{r,total}$ (m^3) is the total reactor volume, $V_{r,dead}$ (m^3) is the reactor dead volume, and V_{sample} (m^3) is the sample volume.

2.5. TOC to CO_2 and CO Conversion. TOC is commonly used as an indicator for the reaction of organic compounds in the HTO process. In fecal sludge, organic carbon mainly appears as solid organic carbon (SOC) and DOC. SOC (e.g., cellulose, proteins) is first hydrolyzed into DOC,[10,11] which is subsequently oxidized to CO_2.[12,13] In our work, CO was detected as the intermediate product of DOC oxidation:

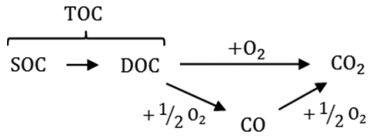

(6)

The evolution of the gaseous reaction products of TOC oxidation, i.e., CO and CO_2, was used as an indicator for TOC conversion. The conversion of TOC was calculated as

$$X_{TOC} = \frac{n_{CO_2} + n_{CO}}{n_{TOC,0}} \quad (7)$$

where n_{CO_2} (mol) and n_{CO} (mol) are moles of CO_2 and CO measured in the product phases, respectively. $n_{TOC,0}$ (mol) is the amount of organic carbon contained in the reactant, calculated by

$$n_{TOC,0} = \frac{w_{TOC}}{100\%} \frac{m_{TS}}{M_C} \quad (8)$$

where w_{TOC} (% by weight) is the mass fraction of TOC in the total solids of the fecal sludge, m_{TS} (kg) is the mass of total solids that was weighed into the reactor prior to the experiment, and M_C (kg mol^{-1}) is the molar mass of carbon.

The molar amount of carbon contained in the product gas in the form of CO_2 and CO was calculated by

$$n_{CO_2} = n_{CO_2,gas} + n_{CO_2,dissolved} = y_{CO_2} \frac{p_{amb} V_{gas}}{R T_{amb}} + \frac{\beta_{DIC} \rho_{liq,prod} m_{liq,prod}}{M_C} \quad (9)$$

$$n_{CO} = n_{CO,gas} = y_{CO} \frac{p_{amb} V_{gas}}{R T_{amb}} \quad (10)$$

$n_{CO_2,gas}$ (mol) and $n_{CO,gas}$ (mol) are the amounts of CO_2 and CO contained in the product gas, respectively, $n_{CO_2,dissolved}$ (mol) is the amount of CO_2 dissolved in the reaction liquid. The amount of CO dissolved in the liquid phase was neglected because of its much lower solubility compared to CO_2. y_{CO_2} (mol$_{CO_2}$ mol$_{gas}^{-1}$) and y_{CO} (mol$_{CO}$ mol$_{gas}^{-1}$) are the molar fractions of CO_2 and CO contained in the product gas measured by gas chromatography, respectively. T_{amb} (K) and p_{amb} (Pa) are the ambient temperature and pressure at the moment of the volume measurement of the gas. T_{amb} was assumed to be 293.15 K, and p_{amb} was assumed to be 0.1013 MPa. V_{gas} (m^3) is the total volume of the product gas. β_{DIC} (kg m^{-3}) represents the mass concentration of DIC measured in the product liquid, $m_{liq,prod}$ (kg) is the mass of the recovered liquid product phase (drained liquid + water detected in the methanol flushing phase), $\rho_{liq,prod}$ (kg m^{-3}) is the liquid product density (estimated as 10^3 kg m^{-3}), and M_C (kg mol^{-1}) is the molar mass of carbon. All DIC contained in the liquid product was assumed to be dissolved CO_2 and/or carbonates originating from the organic fraction of the feces. This assumption is supported by the fact that DIC was only detected in the liquid product when the CO_2 concentration of the product gas was ≥4.5 mol %. Any dissolved CO_2 and carbonates already present in the feces would add to the value of n_{CO_2}. Because the amount of inorganic carbon in the feces is small (approx. 5 % of total C; compare Table 1), this contribution was neglected.

2.6. Approximation of the Reaction Temperature Curves. The main part of the TOC was already decomposed to CO_2 and CO before the reaction temperature had reached steady state (i.e., $T_r = T_{sand}$). The evolution of the reaction temperature T_r (K) with time t (s) of each experiment was approximated by

$$T_r(t) = \begin{cases} T_{steady} + a_{heating} e^{b_{heating} t}; & 0 < t \le \bar{t} \\ T_{steady} + c_{cooling}(t - \bar{t}); & \bar{t} < t < t_{end} \end{cases} \quad (11)$$

where $\bar{t}$ (s) is the retention time of the reactor in the sand bath, t_{end} (s) is the time when the reaction was assumed to have completely stopped ($T_r \le 300$ °C after the reaction). t_{end} defines the overall reaction time ($t_r = t_{end}$). T_{steady} (K), $a_{heating}$ (K), $b_{heating}$ (s^{-1}), and $c_{cooling}$ (K s^{-1}) are constants that were determined by regression of the temperature evolution curves. All parameters were determined individually for each experiment.

3. KINETIC MODELING APPROACHES FOR HYDROTHERMAL FECAL SLUDGE OXIDATION

The experimental data were used to parametrize the four different kinetic reaction models summarized in Table 2.

Model I (eqs 15 and 16) assumes that all TOC is directly decomposed to CO_2 only. Conversion of TOC to CO was not included in this model. The nonuniformity of the TOC decomposition rate (because of the individual reaction rates of different biomass compounds) was taken into account by applying a DAEM. A detailed description of the DAEM (distributed activation energies model) applied to HTO reactions can be found in the work of Vogel et al.[24] The fecal sludge TOC was assumed to consist of j individual compounds that react in j parallel first-order reactions with rate constants k_i to CO_2. The reaction order of oxygen was assumed to be zero. The Arrhenius expression was used for the calculation of the reaction rate constants:

$$(k)_{i,m} = (k_0)_{i,m} e^{-(E)_{i,m}/RT} \quad (12)$$

with k_0 (s^{-1}) being the preexponential factor, E (J mol^{-1}) the activation energy, R (J mol^{-1} K^{-1}) the universal gas constant, and T (K) the reaction temperature (eq 11). i and m are indices for the reaction and model, respectively.

DOI: 10.1021/acs.iecr.6b03084
Ind. Eng. Chem. Res. 2016, 55, 11910−11922

Table 2. Summary of the Kinetic Models Used for Data Fitting

model	reactions considered	rate law expression	eq	adjustable parameters
I	$\mathrm{TOC} + \mathrm{O_2} \xrightarrow{(k_{1,I},\ldots,k_{j,I})} \mathrm{CO_2}$	$\frac{dn_{TOC}}{dt} = -(k_{1,I}n_1 + k_{2,I}n_2 + \ldots + k_{j,I}n_j) = -\sum_{i=1}^{j}[k_{i,I}n_i]$	15	$k_{0,I}$, $E_{0,I}$, σ_I
		$\frac{dn_{CO_2}}{dt} = \sum_{i=1}^{j}[k_{i,I}n_i]$	16	
II	$\mathrm{TOC} + \mathrm{O_2} \xrightarrow{k_{1,II}} \mathrm{CO_2}$, $\mathrm{TOC} + \frac{1}{2}\mathrm{O_2} \xrightarrow{k_{2,II}} \mathrm{CO}$, $\mathrm{CO} + \frac{1}{2}\mathrm{O_2} \xrightarrow{k_{3,II}} \mathrm{CO_2}$	$\frac{dn_{TOC}}{dt} = -k_{1,II}n_{TOC} - k_{2,II}n_{TOC}$	17	$k_{0,1,II}$, $k_{0,2,II}$, $k_{0,3,II}$, $E_{1,II}$, $E_{2,II}$, $E_{3,II}$
		$\frac{dn_{CO}}{dt} = k_{2,II}n_{TOC} - k_{3,II}n_{CO}$	18	
		$\frac{dn_{CO_2}}{dt} = k_{1,II}n_{TOC} + k_{3,II}n_{CO}$	19	
III	$\mathrm{TOC} + 1 + \frac{\beta}{2}\mathrm{O_2} \xrightarrow{k_{1,III}} \beta\mathrm{CO_2} + (1-\beta)\mathrm{CO}$, $\mathrm{O} + \frac{1}{2}\mathrm{O_2} \xrightarrow{k_{CO,III}} \mathrm{CO_2}$	$\frac{dn_{TOC}}{dt} = -k_{1,III}n_{TOC}$	20	$k_{0,1,III}$, $k_{0,CO,III}$, $E_{1,III}$, $E_{CO,III}$, β
		$\frac{dn_{CO}}{dt} = (1-\beta)k_{1,III}n_{TOC} - k_{CO,III}n_{CO}$	21	
		$\frac{dn_{CO_2}}{dt} = \beta k_{1,III}n_{TOC} + k_{CO,III}n_{CO}$	22	
IV	$\mathrm{TOC} + 1 + \frac{\beta}{2}\mathrm{O_2} \xrightarrow{(k_{1,IV},\ldots,k_{j,IV})} \beta\mathrm{CO_2} + (1-\beta)\mathrm{CO}$, $\mathrm{CO} + \frac{1}{2}\mathrm{O_2} \xrightarrow{k_{CO,IV}} \mathrm{CO_2}$	$\frac{dn_{TOC}}{dt} = -\sum_{i=1}^{j}[k_{i,IV}n_i]$	23	$k_{0,IV}$, $k_{0,CO,IV}$, $E_{0,IV}$, σ_{IV}, $E_{CO,IV}$, β
		$\frac{dn_{CO}}{dt} = (1-\beta)\sum_{i=1}^{j}[k_{i,IV}n_i] - k_{CO,IV}n_{CO}$	24	
		$\frac{dn_{CO_2}}{dt} = \beta\sum_{i=1}^{j}[k_{i,IV}n_i] + k_{CO,IV}n_{CO}$	25	

The initial molar amounts of each TOC component at $t = 0$ [that were used to solve the ordinary differential equations (ODEs) (15) and (16)] are given by

$$n_{i,0} = n_{TOC,0} f_0(E)\, dE \tag{13}$$

where $n_{i,0}$ (mol) is the molar amount of a single carbon-containing reactant i in the raw material, $n_{TOC,0}$ (mol) is the molar amount of TOC in the raw material, $f_0(E)$ is the approximated probability density function (PDF), and dE is the normalizing variable (equal to the class width of the distribution). The distribution of activation energies of the fecal sludge TOC was approximated by a Gaussian PDF:

$$f_0(E) = \frac{1}{\sqrt{2\,\pi\,\sigma^2}} e^{-(E-E_0)^2/2\sigma^2} \tag{14}$$

E (J mol^{-1}) is the activation energy of an individual compound i, E_0 (J mol^{-1}) is the mean activation energy of the distribution, and σ^2 (J^2 mol^{-2}) is the variance of the distribution.

Model II (eqs 17−19) assumes that the fecal sludge TOC is decomposed to CO_2 and to CO proceeding as two parallel first-order reactions with individual rate constants $k_{1,II}$ and $k_{2,II}$, respectively. CO is oxidized to CO_2 in a consecutive first-order reaction ($k_{3,II}$). The rate constants were calculated as shown in eq 12. The influence of the oxygen-to-fuel equivalence ratio was neglected in all equations. Two different cases were tested:

(a) All six adjustable kinetic parameters ($k_{0,1,II}$, $k_{0,2,II}$, $k_{0,3,II}$, $E_{1,II}$, $E_{2,II}$, and $E_{3,II}$) were varied during the parameter optimization.

(b) Kinetic parameters for the oxidation of CO to CO_2 ($k_{0,3,II}$ and $E_{3,II}$) were fixed at values published by Helling and Tester,[25] who measured the first-order rate constants for CO oxidation in supercritical water. Only four parameters were varied ($k_{0,1,II}$, $k_{0,2,II}$, $E_{1,II}$, and $E_{2,II}$).

Model III (eqs 20−22) assumes that the fecal sludge TOC decomposes in a simple first-order reaction (rate constant $k_{1,III}$) into a fraction β of CO_2 and a fraction $1-\beta$ of CO. β is assumed to be independent of the reaction conditions (i.e., temperature, oxygen-to-fuel equivalence ratio. etc.). CO is converted to CO_2 in a consecutive first-order reaction ($k_{CO,III}$). The rate constants were calculated as shown in eq 12. The influence of the oxygen-to-fuel equivalence ratio was neglected in all equations.

Model IV (eqs 23−25) assumes that the fecal sludge TOC is decomposed in j parallel first-order reactions (according to the DAEM) into a fraction β of CO_2 and a fraction $1-\beta$ of CO (similar to model III). CO is converted to CO_2 in a consecutive first-order reaction ($k_{CO,IV}$). The rate constants for TOC decomposition ($k_{1,IV}$, $k_{2,IV}$, ..., $k_{j,IV}$) were calculated by eq 12. The initial molar amounts of each TOC compound were calculated by eq 13 assuming a Gaussian distribution of activation energies of the fecal sludge TOC (eq 14). Because of computation performance limits, the total number of TOC compounds was limited to 40 ($j = 40$). The interval width dE was set equal to $\sigma/5$, and the upper and lower boundaries of the PDF of the activation energies were set to $E_0 + 4\sigma$ and $E_0 - 4\sigma$, respectively. The influence of the oxygen-to-fuel equivalence ratio was neglected.

Each of the presented models was best fitted to the experimentally obtained fractions of TOC converted to CO_2 ($\frac{n_{CO_2}}{n_{TOC,0}}$) and CO ($\frac{n_{CO}}{n_{TOC,0}}$) by nonlinear least-squares regression.

DOI: 10.1021/acs.iecr.6b03084
Ind. Eng. Chem. Res. 2016, 55, 11910−11922

The sum of squared errors (SSQ) of the $\frac{n_{CO_2}}{n_{TOC,0}}$ and $\frac{n_{CO_2}}{n_{TOC,0}}$ values were added to form the SSQ value, which was minimized:

$$SSQ = \sum_{i=1}^{n}\left[\left(\frac{n_{CO_2}}{n_{TOC,0}}\right)_{i,experimental} - \left(\frac{n_{CO_2}}{n_{TOC,0}}\right)_{i,calculated}\right]^2 + \sum_{i=1}^{n}\left[\left(\frac{n_{CO}}{n_{TOC,0}}\right)_{i,experimental} - \left(\frac{n_{CO}}{n_{TOC,0}}\right)_{i,calculated}\right]^2 \quad (26)$$

with i being the index of the experimental data point and n the total number of experimental data points used for the fit. Equation 26 was minimized by iterative variation of the adjustable kinetic parameters (see Table 2) using the Simplex algorithm (function *fminsearch* in *MATLAB*) or the Pattern search algorithm (function *patternsearch* in *MATLAB*). Different sets of initial parameter values were tested to increase the certainty that the found minimal SSQ represented a global minimum. For a comparison of the models, the standard error of the estimate (SEE) was calculated by

$$SEE = \sqrt{\frac{SSQ}{n-p}} \quad (27)$$

where n is the total number of experimental data points used for the fit and p the number of adjustable parameters of the model. The ODE systems were solved analytically by transformation into linear functions. If an analytical solution was not possible (models II, III, and IV), the ODE systems were solved numerically using the *ode45* function in *MATLAB*.

4. RESULTS AND DISCUSSION

4.1. Experimental Investigation. *4.1.1. HTO of Fecal Sludge.* Depending on the degree of conversion, a transparent brown-yellowish to colorless liquid reaction product was obtained. A solid fraction was suspended in the liquid reaction product consisting of black or white particles that settled within minutes. In several experiments (V41, V42, V43, Lambda 3, Dilute 1, and Dilute 3; compare Table 3), a sticky coke or tarlike byproduct was obtained. The gas phase contained residual O_2, N_2, CO_2, and CO. Formation of H_2 and CH_4 was not observed in any of the experiments. The results of all performed experiments are reported in Tables 3 and 4.

A rapid reaction start, similar to an ignition, indicated by a reproducible sharp peak in the measured temperature and pressure curves was observed at around 300 °C for experiments where the thermocouple for reaction temperature measurement was situated in the gas phase (Midtemp series; Figure 2 and Table 4). The maximum temperature reached up to 490 °C. Peak temperatures increased with increasing oxygen-to-fuel ratio. Experiments where the temperature was measured in the liquid phase exhibited a similar peak in the pressure curve and a small peak (or no peak at all) in the temperature curve at 300 °C. The temperature and pressure peaks are considered to be caused by a rapid gas-phase reaction. It is supposed that during the heat-up of the reactor (below 300 °C) volatile compounds are formed that ignite in the presence of oxygen. Only a marginal carbon conversion was observed for experiments that were stopped before the ignition temperature was reached (Heiz 13; Table 4). Because no CO, H_2, and CH_4 were detected at these conditions, we assume that some volatile organic compounds (e.g., low-molecular-weight alcohols, aldehydes, carboxylic acids, ketones, etc.) are formed[10] and ignite around 300 °C. The reaction kinetics are only slightly influenced by this (gas-phase) ignition because the temperature rise measured in the liquid phase, which contained the majority of the organic fraction, was very small.

Generally, increasing both the reaction temperature and reaction time increased the conversion of TOC to CO_2. At both tested sand-bath temperatures (360 and 470 °C), around 8% of the TOC was first converted to CO and consecutively oxidized to CO_2. The oxidation rate of CO was considerably influenced by the reaction temperature. At 470 °C sand-bath temperature, all of the TOC and CO was converted to CO_2 after ca. 25 min (1570 s). At 360 °C sand-bath temperature, >99% of the TOC was decomposed, and there was still 6% carbon found as CO after 25 min (Table 4).

Table 3. Results of Batch Experiments: Preliminary Experiments and Variation of the Oxygen-to-Fuel Equivalence Ratio λ and Initial TOC Concentration at Standard Reaction Conditions

				CO_2 and CO yield (%)	
expt label	initial air pressure $p_{air,0}$ (MPa)	initial TOC concentration $c_{TOC,0}$ (mol L^{-1})	oxygen-to-fuel equivalence ratio λ	$\frac{n_{CO_2}}{n_{TOC,0}} \times 100\%$	$\frac{n_{CO}}{n_{TOC,0}} \times 100\%$
Variation of the Oxygen-to-Fuel Equivalence Ratio (T_{sand} = 470 °C, t_r = 306 ± 5 s, and T_{end} = 425 ± 4 °C)					
Lambda 5	10.00[b]	9.8 ± 0.3	0.00	9.7 ± 0.1	1.2 ± 0.0
Lambda 3[a]	10.25	9.8 ± 0.3	1.01 ± 0.05	65 ± 5	7.0 ± 0.5
Lambda 2	12.98	9.8 ± 0.3	1.52 ± 0.08	92 ± 6	5.9 ± 0.4
Lambda 1	10.43	9.8 ± 0.3	1.66 ± 0.08	97 ± 6	5.2 ± 0.4
Lambda 4	10.03	9.8 ± 0.3	1.94 ± 0.10	102 ± 6	6.3 ± 0.4
Variation of the Initial TOC Concentration (T_{sand} = 470 °C, t_r = 302 ± 3s, and T_{end} = 429 ± 3 °C)					
Dilute 4	9.02	7.4 ± 0.3	1.22 ± 0.06	79 ± 5	7.9 ± 0.6
Dilute 5	9.06	6.5 ± 0.2	1.23 ± 0.06	74 ± 5	9.6 ± 0.6
Dilute 2	9.25	5.6 ± 0.2	1.24 ± 0.06	78 ± 5	9.9 ± 0.6
Dilute 1[a]	5.64	5.1 ± 0.2	1.19 ± 0.06	55 ± 4	10.8 ± 0.7
Dilute 3[a]	9.92	3.9 ± 0.1	1.25 ± 0.06	45 ± 3	5.3 ± 0.3
Screening Experiments (T_{sand} = 550 °C and T_{end} = 400 °C)					
V41[a]	5.11	3.5 ± 0.1	0.64 ± 0.03	38	6.7
V42[a]	5.06	3.5 ± 0.1	0.62 ± 0.03	39	6.6
V43[a]	4.98	3.5 ± 0.1	0.62 ± 0.03	37	6.3

[a]Formation of coke and tar observed. [b]Helium used instead of air.

DOI: 10.1021/acs.iecr.6b03084
Ind. Eng. Chem. Res. 2016, 55, 11910−11922

Table 4. Results of Batch Experiments: Variation of the Reaction Time [Initial Air Pressure $p_{air,0}$ = 10.0 MPa, Oxygen-to-Fuel Equivalence Ratio λ = (1.15−1.23) ± 0.06, and Initial TOC Concentration $c_{TOC,0}$ = 9.8 ± 0.3 mol L^{-1}][a]

				CO_2 and CO yield (%)	
expt label	sand-bath temperature T_{sand} (°C)	reaction time t_r (s)	end temperature T_{end}[b] (°C)	$\frac{n_{CO_2}}{n_{TOC,0}} \times 100\%$	$\frac{n_{CO}}{n_{TOC,0}} \times 100\%$
Heiz 13	470	86	237	1.2 ± 0.0	b.d.l.
Heiz 12	474	120	302	8.1 ± 0.6	b.d.l.
Heiz 6	475	138	317	12.2 ± 0.8	b.d.l.
Heiz 5	476	171	358	45 ± 3	4.0 ± 0.3
Heiz 11	473	225	395	68 ± 5	7.4 ± 0.6
Heiz 3	478	230	412	73 ± 6	8.1 ± 0.7
Heiz 7	474	294	424	85 ± 6	6.8 ± 0.5
Heiz 8	472	373	435	88 ± 6	6.5 ± 0.4
Heiz 9	473	418	448	94 ± 7	4.5 ± 0.3
Heiz 4	478	511	464	96 ± 7	2.2 ± 0.2
Heiz 10	473	681	463	97 ± 7	2.1 ± 0.4
Heiz 2	474	1572	469	101 ± 6	b.d.l.
Midtemp 7	362	235	314	27 ± 3	0.0
Midtemp 8	356	261	327	37 ± 2	2.5 ± 0.2
Midtemp 6	365	311	333	66 ± 4	6.2 ± 0.4
Midtemp 5	359	354	323	72 ± 5	6.3 ± 0.4
Midtemp 1	365	527	346	80 ± 5	7.7 ± 0.5
Midtemp 2	360	781	352	89 ± 5	7.6 ± 0.5
Midtemp 9	348	634	353	88 ± 5	6.9 ± 0.4
Midtemp 3	362	1519	364	94 ± 6	5.8 ± 0.4
		Reproducibility Test			
Rep 1	474	303	427	88 ± 6	7.1 ± 0.4
Rep 2	474	309	428	94 ± 6	5.7 ± 0.4
Rep 3	473	304	424	84 ± 5	8.0 ± 0.5
Average				89[c] ± 5[d]	7[c] ± 1[d]

[a]The uncertainties of the calculated values were estimated by uncertainty propagation from analytical values. CO_2 and CO yields from TOC decomposition were calculated using eqs 8−10. b.d.l. = below detection limit. [b]Temperature that was reached when the reactor was removed from the sand bath. [c]Average of Rep 1, Rep 2, and Rep 3. [d]Standard error of Rep 1, Rep 2, and Rep 3.

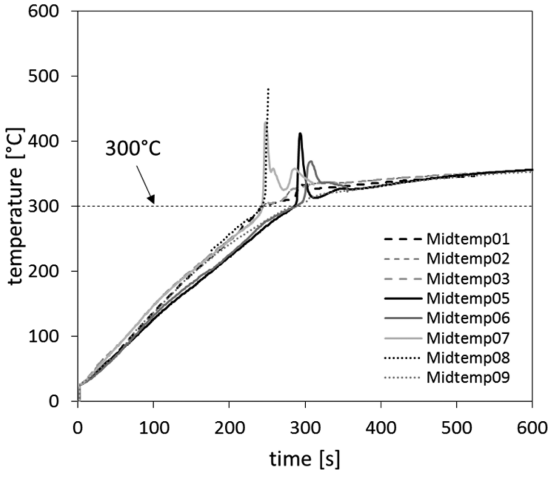

Figure 2. Temperature curves of the experiments where the temperature was measured in the gas phase during heat-up indicating an ignition at around 300 °C.

The reproducibility of TOC conversions was assessed from three reproduced experiments at standard conditions (Rep 1−3 in Table 4) and was around 5% for the TOC to CO_2 conversion and 1% for the TOC to CO conversion. Uncertainties of all conversion data were also estimated by Gaussian uncertainty propagation from measurement uncertainties. The estimated uncertainties at standard conditions (6−7% for the TOC to CO_2 conversion and 0.5% for the TOC to CO conversion; Table 4) are in a range similar to that of uncertainties measured from the reproducibility test. The inaccuracy of gas composition measurement and inhomogeneity of the used feedstock were found to have the greatest influence on the reproducibility.

An increase of the oxygen-to-fuel equivalence ratio λ increased the conversion of TOC to CO_2 (Lambda 1−5 in Table 3). These findings are in accordance with the findings of Goto et al.[26] Formation of CO was insignificantly influenced by an increase of λ.

An increase in the feces dilution (or a decrease in the feed concentration) slightly decreased the conversion of TOC to CO_2 and slightly increased the TOC to CO conversion in those experiments where no coke and tar was formed (Dilute 2, 4, and 5; Table 3 and Figure 3). When coke and tar were formed (Dilute 1 and 3), the conversion of TOC to CO_2 was considerably lower.

Several authors reported a first-order dependence of the rate of TOC disappearance on the reactant concentration (i.e., TOC conversion is independent of the initial TOC concentration) for HTO of biomasses that are similar to fecal sludge, e.g., municipal sewage sludge,[4] dog food waste,[27] or biological sludge.[28] We tested whether the observed increase of conversion with the initial TOC concentration of our results (Figure 3) was statistically significant. An F test[29] was performed including values Dilute 2, 3, and 5 and Rep 1−3 (n = 6). Values that were associated with coke and tar formation (Dilute 1 and 3) were not considered for the test. The test was based on the null hypothesis that there was no significant linear trend (p = 2). At a level of

DOI: 10.1021/acs.iecr.6b03084
Ind. Eng. Chem. Res. 2016, 55, 11910−11922

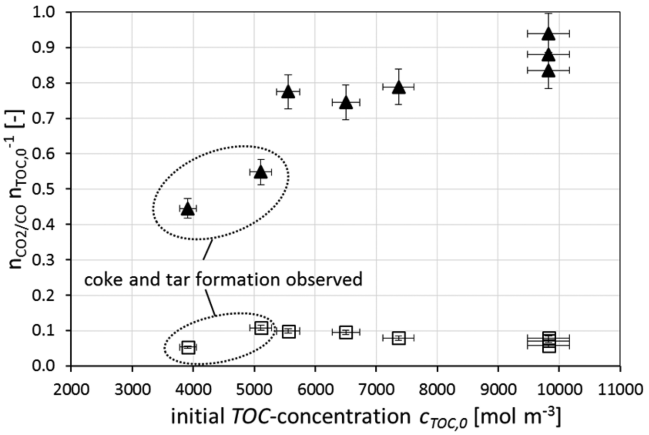

Figure 3. TOC to CO_2 (▲) and TOC to CO (□) conversion for various fecal sludge dilutions measured at standard conditions (T_{sand} = 470 °C, t_r = 300 s, and λ = 1.2).

confidence of α = 5%, the null hypothesis was not rejected for both TOC to CO_2 and TOC to CO conversion. The increase of conversion with increasing TOC concentration is thus not supposed to be significant. This result justifies the assumption of a first-order dependence on the reactant concentration of the reaction rates for TOC disappearance in our work.

When our data are compared to those of Price,[15] Goto et al.,[4] and Shanableh and Gloyna[30] for other biological sludges, we find similar conversions of carbon at comparable reaction conditions. Price[15] observed minor formation of CH_4 and H_2, aside from CO_2 and CO in their product gas. Miller and co-workers[19] found that the solids concentration of the feed had an influence on the temperature increase of the reaction. This could also provide an explanation for the slightly lower conversions observed for the experiments with a lower initial TOC content.

4.1.2. CO Formation and Subsequent Oxidation to CO_2. Little is known about the formation of CO from biological sludges under HTO conditions. Four main routes are conceivable:

(a) All organic carbon reacts first with oxygen to CO, which is then further oxidized to CO_2 in a consecutive reaction. CO would thus be the primary product and CO_2 the secondary one.

(b) CO is formed from the organic carbon in an independent reaction (with or without the involvement of oxygen), parallel to the formation of CO_2 from the organic carbon (eq 6). Both CO and CO_2 would then be primary products.

(c) CO is formed from CO_2 and solid carbon in a Boudouard-type equilibrium reaction: $CO_2 + C \leftrightarrow 2CO$.

(d) CO is formed via the reverse water−gas shift reaction: $CO_2 + H_2 \leftrightarrow CO + H_2O$.

Our data support route b because the CO yield increases later than the CO_2 yield (Table 4). For route a, the CO yield would increase first, followed by an increase of CO_2. Furthermore, in route a, a lack of oxygen (λ < 1) would result in large amounts of CO in the product gas. The highest CO concentration of 1.3 vol % was obtained in experiment V41 with λ = 0.6, along with a CO_2 concentration of 7.1 vol %. This carbon distribution is not compatible with that of route a for λ = 0.6, which would just be enough to convert all carbon to CO and only a small fraction further to CO_2; i.e., the CO concentration should in that case be much higher than the CO_2 concentration.

Route c is implausible because the high pressures in our experiments drive the equilibrium to the reactants, CO_2 and C. Because no solid carbon was found in most of the experiments, this pathway seems unlikely to have contributed significantly to the formation of CO. Route d is also dropped because CO would once more be a secondary product from CO_2 and thus exhibit a different trend. Furthermore, significant amounts of hydrogen would have to be formed first to drive this reaction toward CO and water.

Only a little formation of CO, i.e., 0.13 vol % or 10 times less than that for λ = 0.6, was observed under oxygen-free conditions (λ = 0). This suggests that oxygen is needed for the formation of CO from the organic carbon. The most probable explanation for CO formation is decarbonylation of organic intermediates, formed by the partial oxidation of organic carbon. Acetaldehyde is known to form CO under hydrothermal conditions.[31] Another likely candidate is formic acid. It is formed as an intermediate during HTO of sewage sludge.[26] It was further shown[32] to decompose to CO and H_2O and to CO_2 and H_2. Because hydrogen was not detected in any of our experiments, decomposition of formic acid to CO and water would be another plausible source for some of the measured CO.

4.1.3. Coke and Tar Formation. Coke and tar were formed especially when the $p-T$ trajectory of an experiment crossed the vapor pressure curve of water (Figure 4). This happened, for

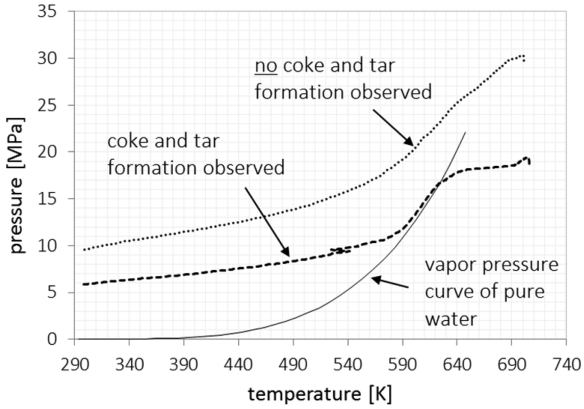

Figure 4. Measured $p-T$ curves of exemplary experiments Dilute 1 with intersection (---) and Dilute 2 without intersection (···) of the vapor pressure curve of pure water. λ was 1.2 in both experiments.

example, when a low initial air pressure was applied or when the reactor loading was increased by the addition of water for dilution (experiments Dilute 1 and 3).

Tars are ill-defined high-molecular-weight compounds, and coke is a carbon-rich solid. Coke and tars are formed by repolymerization of liquefied organic compounds during thermal decomposition of biomass. Compared to other biomass compounds, both tar and coke are slowly decomposed during thermal treatment.[33] They are formed as byproducts of hydrothermal gasification processes[34] and of pyrolysis and dry gasification,[33] where no oxygen or only limited oxygen is available. In experiment Lambda 5 of this study, where no air was supplied (λ = 0; compare Table 3), no tar and coke formation occurred. At a λ value slightly below 1, tars and coke were formed (Lambda 3). These observations do not paint a clear picture of the reasons for coke and tar formation in our experiments. One explanation for coke and tar formation is that when the vapor pressure curve of water is intersected, all liquid water is vaporized, forming a "dry" biomass phase in the reactor. Because of the high reactor temperatures and slow reaction of oxygen with solid biomass, the biomass would be pyrolyzed, forming tars and coke.

DOI: 10.1021/acs.iecr.6b03084
Ind. Eng. Chem. Res. 2016, 55, 11910−11922

Table 5. Summary of the Obtained Best-Fit Model Parameters

	preexponential factor			activation energy						
model	$k_{0,1}$ (s^{-1})	$k_{0,2}$ (s^{-1})	$k_{0,3}$, $k_{0,CO}$ (s^{-1})	E_0, E_1 (kJ mol^{-1})	E_2 (kJ mol^{-1})	E_3, E_{CO} (kJ mol^{-1})	σ (kJ mol^{-1})	β	SSQ	SEE[b]
I	36.13			43			3.8		0.0969	0.0696
IIa	24.95	8.93	77253	40	46	101			0.0730	0.0427
IIb	11.74	61.26	316000[a]	37	54	112[a]			0.1335	0.0578
III	19.82		66122	39		101		0.907	0.0739	0.0424
IV	24.7		477765	39		113	2.2	0.907	0.0943	0.0485

[a]Fixed values published by Helling and Tester.[25] [b]Calculation basis: model I, 23 data points (CO_2 only); models II–IV, 46 data points (CO_2 and CO).

The exact reasons for the formation of coke and tars were not further investigated in this study. Their formation can be avoided by applying a low ratio of water to air, i.e., a high initial air pressure and a small amount of water (water contained in the fecal sludge plus water added for dilution). The data points from experiments where tar and coke formation occurred were not included in the kinetic analysis.

4.2. Kinetic Analysis. *4.2.1. Kinetic Modeling of Hydrothermal Fecal Sludge Oxidation.* The obtained conversion results from Table 4 were used for kinetic modeling. Data points from Table 3 were not included in the kinetic study.

Models I–III (Table 2) showed quick convergence when the Simplex algorithm (*fminsearch*) was used. Model IV only reached a global minimum when the Pattern search algorithm was used. Convergence was relatively slow because of a high number of iteration steps. Model I did not converge to a global minimum if only data points from experiments conducted at 470 °C sand-bath temperature were used (Heiz series). Only local minima were found, resulting in implausible parameter values (e.g., activation energies of >200 kJ mol^{-1}).

Best-fit activation energies (models II and III) and mean activation energies (models I and IV), respectively, for TOC to CO_2 decomposition between 37 and 43 kJ mol^{-1} were obtained (Table 5). Best-fit activation energies for TOC to CO decomposition were slightly higher, between 46 and 54 kJ mol^{-1}. Models I and IV using the DAEM gave best-fit σ values between 2.2 and 3.8 kJ mol^{-1}. Models that included CO to CO_2 oxidation (II–IV) yielded activation energies between 101 and 110 kJ mol^{-1} for this reaction. Models III and IV that assumed a fractional TOC decomposition into CO_2 and CO yielded a best-fit β value of 0.907.

The highest prediction accuracy was achieved by model III (SEE = 0.0424; Table 5). The model curves smoothly fit the CO_2 and CO data points over the whole reaction time (Figure 5, model III). TOC-to-CO_2 conversion is slightly underpredicted at 360 °C sand-bath temperature (t_r = 300–400 s) and slightly overpredicted at 470 °C sand-bath temperature (t_r = 120–150 s). Model IIa achieves almost the same prediction accuracy (SEE = 0.0427) and exhibits similar deviations at the same retention times as model III. The prediction of model IV is slightly less accurate (SEE = 0.0485) despite its use of the DAEM. Models I and IIb showed the lowest prediction accuracy (higher SEE) compared to the other models, especially for TOC-to-CO_2 conversions of >90%.

The model prediction accuracy was slightly increased by increasing the model complexity (e.g., increase of the considered reaction paths) and the number of adjustable parameters. However, the use of DAEM did not increase the model accuracy. All models exhibit similar activation energies for TOC decomposition to CO_2 in the range of 37–43 kJ mol^{-1}, regardless of the model approach used, underlining the plausibility of the obtained values.

The lack of accuracy of model I is assumed to be caused by the neglected formation of CO. Because CO reacts relatively slowly, especially at lower reaction temperatures, the prediction becomes inaccurate after the main part of the TOC is decomposed (Figure 5, model I).

The activation energies for CO oxidation to CO_2 in models IIa and III (101 and 101 kJ mol^{-1}, respectively) are slightly lower than the value reported by Helling and Tester[25] (112 kJ mol^{-1}). Vice versa, model IIb that uses this literature value exhibits a low prediction accuracy for longer retention times and higher conversions (Figure 5, model IIb). On the other hand, model IV exhibits an activation energy for CO oxidation (113 kJ mol^{-1}) similar to the reported literature value of E_{CO}. This indicates that the DAEM approach of model IV leads to an increase in the robustness of the model because it results in parameter values similar to accurately determined kinetic data for the single reaction of CO to CO_2.

The β values obtained for models III and IV indicate that ca. 91% of TOC is converted to CO_2 and 9% of TOC is converted to CO in parallel reaction paths.

The oxygen-to-fuel equivalence ratio λ had a small influence on the rate of TOC conversion in the range of λ values studied, i.e., 1.2–1.9, with higher λ leading to a higher TOC conversion. We tried to include this influence in our kinetic models, with unsatisfactory results. The influence on TOC conversion was not well captured and extrapolation to λ values of <1 led to an unrealistic formation of CO. Thus, we decided to exclude any influence of λ on the rates of reaction in our models.

4.2.2. Comparison of the Observed Conversion Results with the Literature Data. TOC conversions observed in this work were plotted against the predictions made by model III (Figure 6).

Additionally, model III was used to calculate conversions using the experimental conditions (t and T) published by other authors[26,27,30] and plotted against the conversions observed in those studies in the same figure.

Model III fits the experimental conversions of this work well except for experiments that are associated with coke and tar formation. This indicates that the model has poor validity if coke and tar are formed during the reaction because these products are not accounted for in the kinetic scheme. Model III shows a poor fit upon predictions of the conversions of municipal sewage sludge[26] and dog food.[27] TOC conversions of these substrates are generally underpredicted by the model. The prediction of model III for activated sludge[30] is accurate when conversions at reaction temperatures of 400–450 °C are predicted. The fit for conversions at 300 and 343 °C is poor.

The following activation energies for global first-order reaction models for TOC or COD conversions were reported by the

DOI: 10.1021/acs.iecr.6b03084
Ind. Eng. Chem. Res. 2016, 55, 11910–11922

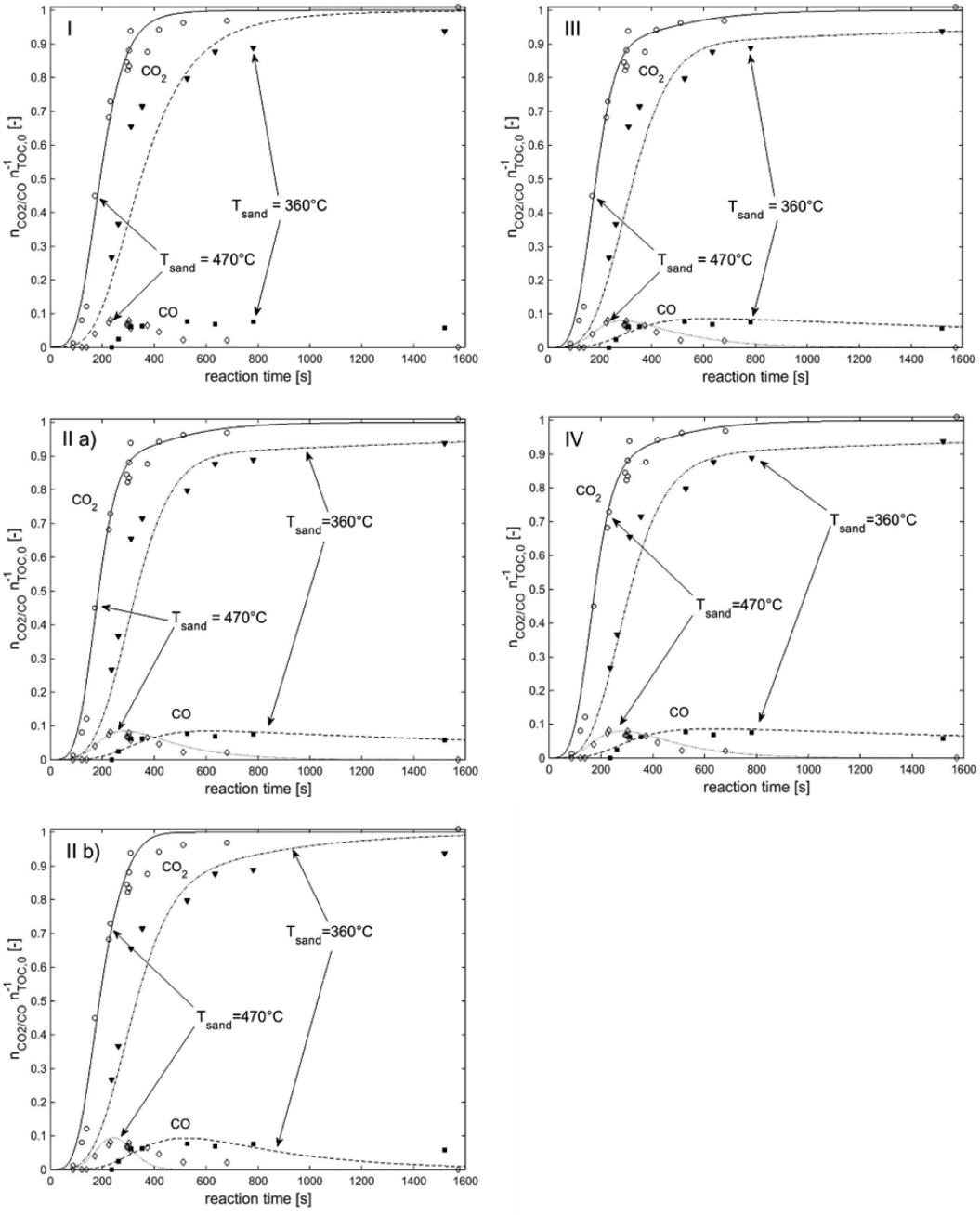

Figure 5. Conversion of TOC to CO_2 and CO over reaction time: experimental data (symbols) from Table 4 and model predictions (lines) using best-fit parameters from Table 2 for the four models I–IV.

other authors: 76 kJ mol^{-1} (TOC) for supercritical water oxidation of municipal sewage sludge,[4] 67 kJ mol^{-1} (COD) for wet oxidation of biological sludge[5] (not shown in Figure 6), 54 kJ mol^{-1} (COD) for wet oxidation of activated sludge,[28] and 97 kJ mol^{-1} (TOC) for supercritical water oxidation of dog food.[27] The activation energies for TOC decomposition obtained in this study, between 37 and 43 kJ mol^{-1}, are lower than these literature values. This explains the poor prediction of model III for some of the experimental points for other substrates in Figure 6.

The most obvious explanation would be that all of these sludges exhibit a different reactivity during HTO. Different ratios of the main constituents, i.e., carbohydrates, proteins, lipids, etc., lead to different overall reactivities. A further reason for the deviations could be that the sludges used in the other studies underwent a pretreatment (e.g., aerobic/anaerobic digestion). Easily degradable compounds would be eliminated by these pretreatment steps, causing a change of the overall activation energy in a global kinetic model. However, Shanableh and Imteaz[35] showed that anaerobic sludge treatment had almost no influence on the first-order HTO reaction kinetics, i.e., activation energy. Another reason for the deviations is the limited range of λ values, i.e., around 1.2, used in our experiments, whereas values as high as 2 were used in the other studies. The influence of the oxygen concentration on the reaction rates should thus be incorporated into the rate expressions of the kinetic model in future work.

Furthermore, important contributions to the deviations between our model predictions and the data of other authors shown in Figure 6 are the different methods for calculating conversion. While in our study conversion is calculated from the CO and CO_2 formed,

DOI: 10.1021/acs.iecr.6b03084
Ind. Eng. Chem. Res. 2016, 55, 11910−11922

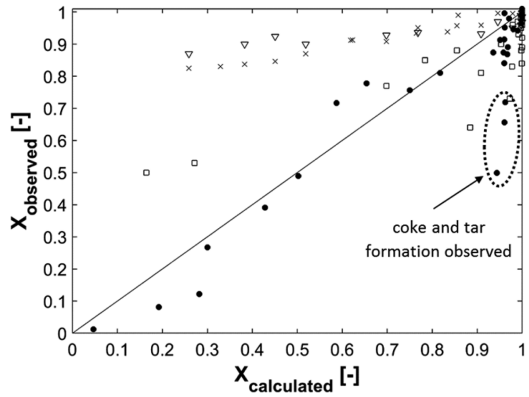

Figure 6. Comparison of the observed and calculated TOC (or COD) conversions using model III with best-fit parameters (Table 5) at given reaction conditions: this study [●; $X_{TOC} = (n_{CO_2} + n_{CO})/n_{TOC,0}$, T < 470 °C, and λ = 0−1.9], municipal sewage sludge[4] (×; $X_{TOC} = 1 - n_{TOC,end}/n_{TOC,0}$, unstirred batch reactor, T = 400−500 °C, and λ = 2.0), activated sludge[30] (□; $X_{COD} = 1 - n_{COD,end}/n_{COD,0}$), unstirred batch reactor, T = 300−450 °C, and λ = 2.1), and dog food waste[27] (∇; $X_{TOC} = 1 - n_{TOC,end}/n_{TOC,0}$, unstirred batch reactor, and λ = 2.0).

the unconverted TOC or COD was used in other studies. Depending on how the samples were drawn and worked up, small solid particles suspended in the solution would not be included in the TOC or COD analysis. We have compared some of our conversion data using the method with CO and CO_2 versus the method with the unconverted DOC and found a significant difference, on the same order of magnitude as the differences shown in Figure 6. It is therefore important to apply our model for predicting conversion data corresponding to CO and CO_2 yields and not to unconverted carbon in the liquid phase.

Vogel et al.[24] used the data of Goto et al.[4] (SCWO of municipal sewage sludge) and adjusted a DAEM using a Gaussian PDF. A mean activation energy for TOC decomposition of 29 kJ mol^{-1} and a σ value of 10.9 kJ mol^{-1} were obtained. The two models using the DAEM approach in this study (models I and IV) exhibit a relatively small breadth of the PDF with σ values of 2.2 and 3.8 kJ mol^{-1}. A detailed analysis of the reaction intermediates would be needed to understand the relatively narrow range of reactivities during HTO of feces. Because of this narrow range, the models with a single reaction approach for TOC decomposition (models II and III) are able to predict the experimental data with an accuracy similar to that of the models using a DAEM.

4.3. Influence of the Rate of Oxygen Mass Transfer on the Measured Reaction Rate. At conditions below the critical point of water (T < 374 °C and p < 22.1 MPa), the majority of oxidation reactions are supposed to occur in the liquid phase among dissolved compounds. Because the reactor content was not agitated, oxygen had to diffuse from the gas phase into the liquid phase to be able to react with the organic material. Thus, the measured reaction rates might be limited by the oxygen mass-transfer rate. At supercritical conditions, the components are assumed to be completely mixed in a single-phase, homogeneous fluid because of the complete miscibility of organic compounds and gases with supercritical water.[36] Therefore, oxygen transport should not play a role. To ensure that the measured reaction rates were not limited by the oxygen transport at subcritical conditions, the oxygen mass-transfer rate was estimated using literature values and compared to the observed rate of oxygen disappearance.

The hypothesis of oxygen-transport limitation can be rejected if the following condition is fulfilled:

$$\left(\frac{dn_{O_2}}{dt}\right)_{measured} < \left(\frac{dn_{O_2}}{dt}\right)_{transport,max} \quad (28)$$

$(dn_{O_2}\ dt^{-1})_{measured}$ ($mol_{O_2}\ s^{-1}$) is the rate of oxygen disappearance, consumed for the reaction of TOC to CO_2, which was calculated using kinetic model I. $(dn_{O_2}\ dt^{-1})_{transport,max}$ ($mol_{O_2}\ s^{-1}$) is the maximum oxygen mass-transfer rate from the gas phase to the liquid phase. According to the two-film theory, the oxygen mass-transfer rate is calculated by

$$\left(\frac{dn_{O_2}}{dt}\right)_{transport} = k_L a(T)\ (c_{O_2}{}^* - c_{O_2}) V_{H_2O}(p, T) \quad (29)$$

$k_L a$ [s^{-1}] is the volume-specific oxygen mass-transfer coefficient, $c_{O_2}{}^*$ (mol m^{-3}) is the oxygen concentration at the liquid−gas-phase boundary, c_{O_2} (mol m^{-3}) is the oxygen concentration in the reacting phase, and V_{H_2O} (m^3) is the volume of the reacting phase depending on the reactor temperature and pressure. For simplification, the reacting phase (fecal sludge) was considered to be pure water. The oxygen concentration at the liquid−gas interface, $c_{O_2}{}^*$, was taken as the oxygen solubility in water calculated with Henry's law.[37] To determine the maximum oxygen mass-transfer rate, a fast reaction in the liquid phase was assumed, leading to $c_{O_2} = 0$.

$k_L a$ was estimated using a correlation determined by Foussard:[38]

$$k_L a(T) = (k_L a)_{T_{ref}} e^{2740 \pm 120K(1/T_{ref} - 1/T)} \quad (30)$$

where $(k_L a)_{T_{ref}}$ (s^{-1}) is the $k_L a$ value at a reference temperature T_{ref} (K; experimental values of 0.003 s^{-1} and 293 K from Foussard's work were used as reference values, respectively) and T (K) is the temperature. Foussard[38] measured $k_L a$ values of oxygen in a cylindrical stirred batch reactor in a temperature range between 20 and 240 °C at stirrer speeds between 100 and 800 min^{-1}. For this study, eq 30 was extrapolated to 374 °C and to a rotational speed of 0 min^{-1}, i.e., no mixing. The obtained $k_L a$ values were corrected by dividing $k_L a$ by the volume-specific surface area of the reactant [a (m^{-1}) = liquid−gas interface (m^2)/liquid volume (m^3)] used in Foussard's work and multiplying it by the volume-specific surface area of the reactant used in this study.

The highest oxygen reaction rates were observed in the experiments conducted at 470 °C sand-bath temperature. Between the reaction start at around 300 °C and before the critical point of water (374 °C) is reached, fast oxidation reactions occur in the two-phase system, indicated by the high TOC conversion rates. In this region, the calculated oxygen mass-transfer rate is higher than the oxygen reaction rate (Figure 7). Below ca. 280 °C, the oxygen mass-transfer rate is smaller than the measured rate of oxygen consumption. Because at these temperatures almost no conversion of TOC takes place, the influence of oxygen transport on the kinetic parameters is minimal.

5. CONCLUSION

TOC contained in fecal sludge is decomposed to CO_2 and CO as within minutes in supercritical water in the presence of stoichiometric amounts of oxygen at temperatures below 480 °C.

DOI: 10.1021/acs.iecr.6b03084
Ind. Eng. Chem. Res. 2016, 55, 11910−11922

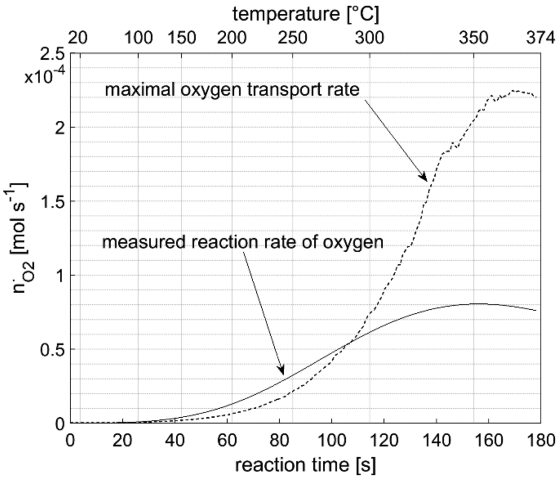

Figure 7. Oxygen reaction rate (measured rate of disappearance) and calculated maximal oxygen mass-transfer rate versus reaction time (T_{sand} = 470 °C, and standard reaction conditions). The upper abscissa shows the corresponding reactor temperature.

CO is suggested to be formed by decarbonylation of organic compounds, such as acetaldehyde or formic acid, independent from CO_2. The reaction temperature and oxygen-to-fuel equivalence ratio affect the decomposition rate of TOC most. Dilution of fecal sludge has no significant effect on the conversion. Formation of coke and tar observed under certain reaction conditions is avoided by adjusting the reaction conditions (amount of water in the reactor and initial air pressure). A limitation of the measured reaction rates by oxygen mass transfer is ruled out.

The proposed reaction models II–IV are able to accurately model the TOC decomposition indicated by CO and CO_2 evolution with a reasonable level of model complexity. Neglecting CO formation (model I) is an oversimplification that is only acceptable for high temperatures and long reaction times. The use of the DAEM approach increases the model complexity and number of adjustable parameters. The prediction accuracy is not increased significantly for the range of conversions studied because the breadth of reactivities in fecal sludge is small.

A further improvement of the model's ability to predict a wider range of operating conditions should include experimental data at higher temperatures (>470 °C) and higher oxygen-to-fuel equivalence ratios (>1.9). The influence of the latter should be analyzed in more detail, and the rate expressions should be extended to include a term for λ or n_{O_2}. Validation of the model predictions with different fecal sludges would also extend the applicability of this work.

AUTHOR INFORMATION

Corresponding Author

*Tel.: +41-56-202-7334. E-mail: frederic.vogel@fhnw.ch.

Notes

The authors declare no competing financial interest.

ACKNOWLEDGMENTS

We kindly acknowledge the laboratory and technical assistance of Timon Käser, Thanh-Binh Truong, Erich De Boni, and Lorenz Bäni. We thank Mr. Schneider from the Laboratory for Organic Chemistry, ETH Zürich, for CHONS analyses. We also thank Kai Udert, EAWAG, for valuable discussions and his continuing support. We thank Rahel Künzle, EAWAG, for collecting and providing fecal sludge. This work was performed within the Blue Diversion Autarky project funded by the Bill & Melinda Gates Foundation (Seattle, WA) via a subgrant from EAWAG.

REFERENCES

(1) WHO. Progress on Sanitation and Drinking-Water: 2013 Update; 2013.

(2) Brunner, G. Near and Supercritical Water. Part II: Oxidative Processes. *J. Supercrit. Fluids* **2009**, *47*, 382–390.

(3) Gloyna, E. F.; Li, L. Supercritical Water Oxidation: An Engineering Update. *Waste Manage.* **1993**, *13*, 379–394.

(4) Goto, M.; Nada, T.; Kodama, A.; Hirose, T. Kinetic Analysis for Destruction of Municipal Sewage Sludge and Alcohol Distillery Wastewater by Supercritical Water Oxidation. *Ind. Eng. Chem. Res.* **1999**, *38*, 1863–1865.

(5) Foussard, J.; Debellefontaine, H.; Besombes-Vailhé, J. Efficient Elimination of Organic Liquid Wastes: Wet Air Oxidation. J. Environ. *J. Environ. Eng.* **1989**, *115*, 367–385.

(6) Mishra, V. S.; Mahajani, V. V.; Joshi, J. B. Wet Air Oxidation. *Ind. Eng. Chem. Res.* **1995**, *34*, 2–48.

(7) Pruden, B. B.; Le, H. Wet Air Oxidation of Soluble Components in Waste Water. *Can. J. Chem. Eng.* **1976**, *54*, 319–325.

(8) Jönsson, H.; Baky, A.; Jeppsson, U.; Hellström, D.; Kärrman, E. *Composition of Urine, Faeces, Greywater and Biowaste for Utilisation in the URWARE Model*; Chalmers University of Technology: Gothenburg, Sweden, 2005.

(9) Rose, C.; Parker, A.; Jefferson, B.; Cartmell, E. The Characterization of Feces and Urine: A Review of the Literature to Inform Advanced Treatment Technology. *Crit. Rev. Environ. Sci. Technol.* **2015**, *45*, 1827–1879.

(10) Mochidzuki, K.; Sakoda, A.; Suzuki, M. Liquid-Phase Thermogravimetric Measurement of Reaction Kinetics of the Conversion of Biomass Wastes in Pressurized Hot Water: A Kinetic Study. *Adv. Environ. Res.* **2003**, *7*, 421–428.

(11) Shanableh, A.; Jomaa, S. Production and Transformation of Volatile Fatty Acids from Sludge Subjected to Hydrothermal Treatment. *Water Sci. Technol. J. Int. Assoc. Water Pollut. Res.* **2001**, *44*, 129–135.

(12) Holgate, H. R.; Meyer, J. C.; Tester, J. W. Glucose Hydrolysis and Oxidation in Supercritical Water. *AIChE J.* **1995**, *41*, 637–648.

(13) Jin, F.-M.; Kishita, A.; Moriya, T.; Enomoto, H. Kinetics of Oxidation of Food Wastes with H_2O_2 in Supercritical Water. *J. Supercrit. Fluids* **2001**, *19*, 251–262.

(14) Li, L.; Chen, P.; Gloyna, E. F. Generalized Kinetic Model for Wet Oxidation of Organic Compounds. *AIChE J.* **1991**, *37*, 1687–1697.

(15) Price, C. M. Wet Oxidation of Human Waste. Master Thesis, Massachusetts Institute of Technology, Cambridge, MA, 1981.

(16) Takahashi, Y. Water Oxidation Waste Management System for a CELSS -The State of the Art. *Biol. Sci. Space* **1989**, *3*, 45–54.

(17) Takahashi, Y.; Nitta, K.; Ohya, H.; Oguchi, M. The Applicability of Catalytic Wet-Oxidation to Celss. *Adv. Space Res.* **1987**, *7*, 81–84.

(18) Jagow, R. B. *A Study to Evaluate the Feasibility of Wet Oxidation for Shipboard Waste Water Treatment Application*; Department of Transportation: Washington, DC, 1975.

(19) Miller, A.; Espanani, R.; Junker, A.; Hendry, D.; Wilkinson, N.; Bollinger, D.; Abelleira-Pereira, J. M.; Deshusses, M. A.; Inniss, E.; Jacoby, W. Supercritical Water Oxidation of a Model Fecal Sludge without the Use of a Co-Fuel. *Chemosphere* **2015**, *141*, 189–196.

(20) Sluiter, A.; Hames, B.; Ruiz, R.; Scarlata, C.; Sluiter, J. *Determination of Ash in Biomass*; National Renewable Energy Laboratory, U.S. Department of Energy, Office of Energy Efficiency and Renewable Energy, Golden, CO, 2008; pp 1–5.

(21) Zöhrer, H. Hydrothermal Gasification of Fermentation Residues for SNG-Production. Dissertation, ETH Zürich, Zürich, Switzerland, 2013.

(22) Helling, R. K.; Tester, J. W. Oxidation of Simple Compounds and Mixtures in Supercritical Water: Carbon Monoxide, Ammonia and Ethanol. *Environ. Sci. Technol.* **1988**, *22*, 1319–1324.

DOI: 10.1021/acs.iecr.6b03084
Ind. Eng. Chem. Res. 2016, 55, 11910–11922

(23) Cruciani, G.; Atkins, P. W. *Kurzlehrbuch Physikalische Chemie*; John Wiley & Sons: New York, 2006.
(24) Vogel, F.; Smith, K. A.; Tester, J. W.; Peters, W. A. Engineering Kinetics for Hydrothermal Oxidation of Hazardous Organic Substances. *AIChE J.* **2002**, *48*, 1827−1839.
(25) Helling, R. K.; Tester, J. W. Oxidation Kinetics of Carbon Monoxide in Supercritical Water. *Energy Fuels* **1987**, *1*, 417−423.
(26) Goto, M.; Nada, T.; Kawajiri, S.; Kodama, A.; Hirose, T. Decomposition of Municipal Sludge by Supercritical Water Oxidation. *J. Chem. Eng. Jpn.* **1997**, *30*, 813−818.
(27) Mizuno, T.; Goto, M.; Kodama, A.; Hirose, T. Supercritical Water Oxidation of a Model Municipal Solid Waste. *Ind. Eng. Chem. Res.* **2000**, *39*, 2807−2810.
(28) Shanableh, A. Subcritical and Supercritical Water Oxidation of Industrial Excess Activated Sludge. Dissertation, Department of Civil Engineering, University of Texas, Austin, Austin, TX, 1990.
(29) Ruckstuhl, A.; Stahel, W. Nichtlineare Regression. *Numerische und statistische Methoden für Chemieingenieure*; ETH Zürich and Zürcher Hochschule Winterthur, Zürich, Switzerland, 2008.
(30) Shanableh, A.; Gloyna, E. F. Supercritical Water Oxidation - Wastewaters and Sludges. *Water Sci. Technol.* **1991**, *23*, 389−398.
(31) Arita, T.; Nakahara, K.; Nagami, K.; Kajimoto, O. Hydrogen Generation from Ethanol in Supercritical Water without Catalyst. *Tetrahedron Lett.* **2003**, *44*, 1083−1086.
(32) Yu, J.; Savage, P. E. Decomposition of Formic Acid under Hydrothermal Conditions. *Ind. Eng. Chem. Res.* **1998**, *37*, 2−10.
(33) Fjellerup, J.; Ahrenfeldt, J.; Henriksen, U. *Formation, Decomposition and Cracking of Biomass Tars in Gasification*; Department of Mechanical Engineering, Technical University of Denmark, Lyngby, Denmark, 2005; p 60.
(34) Müller, J. B.; Vogel, F. Tar and Coke Formation during Hydrothermal Processing of Glycerol and Glucose. Influence of Temperature, Residence Time and Feed Concentration. *J. Supercrit. Fluids* **2012**, *70*, 126−136.
(35) Shanableh, A.; Imteaz, M. First-Order Hydrothermal Oxidation Kinetics of Digested Sludge Compared with Raw Sludge. *Environ. Technol.* **2008**, *29*, 1009−1020.
(36) Harvey, A. H.; Friend, D. G. Physical Properties of Water. *Aqueous systems at elevated temperatures and pressures - physical chemistry in water, steam and hydrothermal solutions*; Elsevier: New York, 2004.
(37) Ji, X.; Yan, J. Saturated Thermodynamic Properties for the Air−water System at Elevated Temperatures and Pressures. *Chem. Eng. Sci.* **2003**, *58*, 5069−5077.
(38) Foussard, J. N. Etude de l'oxydation en phase aqueuse à température et à pression élevées: transfert de l'oxygène moléculaire et cinétique de dégradation des acides carboxyliques légers. Dissertation, Institute de Sciences Appliquées, Toulouse, France, 1983.

DOI: 10.1021/acs.iecr.6b03084
Ind. Eng. Chem. Res. 2016, 55, 11910−11922